Supporting information for

Fire and mechanical properties of DGEBA-based epoxy resin cured with a cycloaliphatic hardener: Combined action of silica, melamine and DOPO-derivative

Aurelio Bifulco[1,2†], Dambarudhar Parida[2†], Khalifah A. Salmeia[2,3], Rashid Nazir[2], Sandro Lehner[2], Rolf Stämpfli[4], Hilber Markus[2], Giulio Malucelli[5,*], Francesco Branda[1,*], Sabyasachi Gaan[2,*]

[1]*Department of Chemical Materials and Industrial Production Engineering (DICMaPI) University of Naples Federico II, Naples, Italy*

[2]*Laboratory for Advanced Fibers, Empa Swiss Federal Laboratories for Materials Science and Technology, Lerchenfeldstrasse 5, 9014 St. Gallen, Switzerland*

[3]*Department of Chemistry, Faculty of Science, Al-Balqa Applied University, 19117 Al-Salt, Jordan*

[4]*Laboratory for Biomimetic Membranes and Textiles, Empa Swiss Federal Laboratories for Materials Science and Technology, Lerchenfeldstrasse 5, 9014 St. Gallen, Switzerland*

[5]*Department of Applied Science and Technology, Politecnico di Torino, Viale Teresa Michel 5, Alessandria 15121, Turin, Italy*

[†]Authors contributed equally.

Corresponding authors

branda@unina.it
giulio.malucelli@polito.it
sabyasachi.gaan@empa.ch

Table of contents

## S1. Preparation of in-situ silica-epoxy composites

Synthesis of 3-(6-oxidodibenzo[c,e][1,2]oxaphosphinin-6-yl)propenamide (DA)

DOPO (5.40 g, 25 mmol), acrylamide (355 mg, 50 mmol) were placed in a heavy-walled glass vials sealed with aluminum crimp caps fitted with a silicon septum. The glass tube (with an inner diameter of 3 cm and a volume 60 mL) containing the reaction mixtures was sealed with a lid and heated in the microwave oven for 2 h at 120 °C (50 Bar, 1200W) under N_2 atmosphere. The reactions were performed in Synthwave Microwave Single Reaction Chamber provided by MWS MikrowellenSysteme GmbH, Switzerland. The reaction mixture was continuously stirred with a magnetic stirrer during the irradiation. The temperature, pressure and irradiation power were monitored during the course of the reactions. After cooling down, the solids were washed with water and dried in vacuum at 80 °C as white powder with 66% yield. The NMR data and the melting point concur well with the published data [1, 2].

Table S1. Composition and codes of the investigated epoxy samples

| Sample composition	Code
Pristine epoxy resin (100%)	**EPO**
Epoxy resin (83%), DA (17%)	**DA1**
Epoxy resin (77%), DA (23%)	**DA2**
Epoxy resin (91%), melamine (9%)	**Mel**
Epoxy resin (71%), DA (22%), melamine (7%)	**DA2-Mel**
Epoxy resin (98%), silica (2%)	**Si2**
Epoxy resin (75%), DA (23%), silica (2%)	**Si-DA2**
Epoxy resin (89%), melamine (9%), silica (2%)	**Si-Mel**
Epoxy resin (77%), DA (16%), melamine (5%), silica (2%)	**Si-DA-Mel**
Epoxy resin (69%), DA (22%), melamine (7%), silica (2%)	**Si-DA2-Mel**

S2. ATR-FTIR spectroscopy
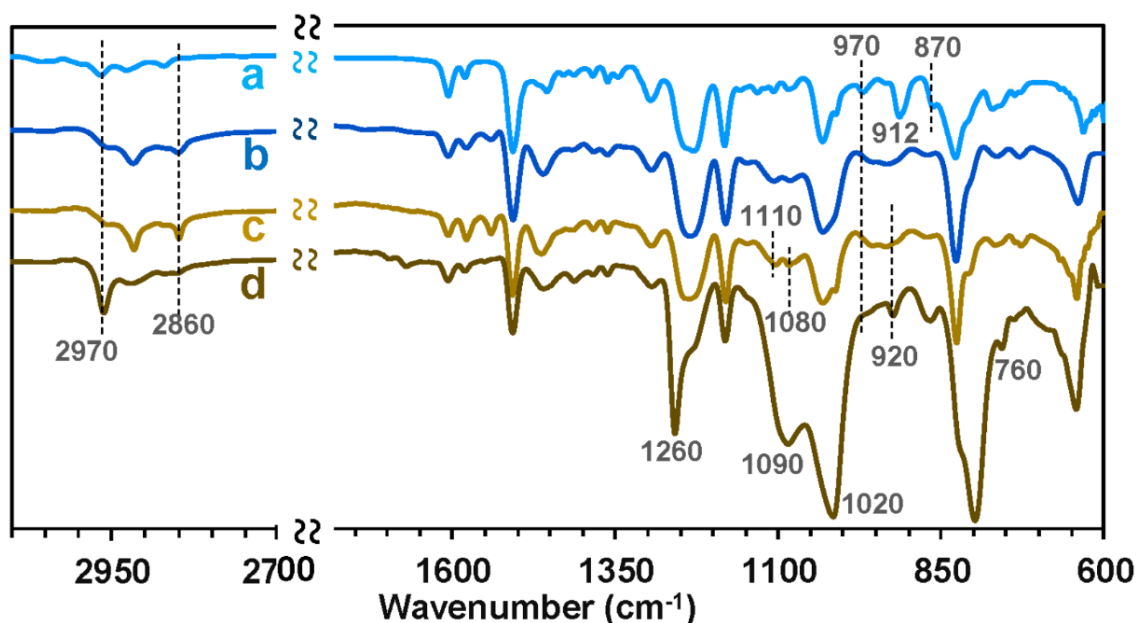
Fig. S1. ATR-FTIR spectra of the uncured resin (a) **EPO_WH**, (b) cured resin **EPO**, (c) in-situ silica-epoxy system **Si2** and (d) in-situ silica-epoxy system containing 2 wt% of P and melamine **Si-DA2-Mel**.

Fig. S1 shows that after addition of the flame retardant additive DA to the in-situ silica-epoxy system (**Si-DA2-Mel**) two strong bands of C–O stretching of amide appeared at 1090 cm^{-1} and 1260 cm^{-1} along with a weak shoulder at 966 cm^{-1} corresponding to P–O–C bonds [3]. The band around 760 cm^{-1} can be attributed to the P–C stretching and the one at 920 cm^{-1} is ascribed to the torsional vibration of the acetaldehyde structure [3]. The bands located between 2860 cm^{-1} and 2970 cm^{-1} can be attributed to the stretching vibration of the C–H and the band around 800 cm^{-1} refers to the bending vibration of the N–H bond which presents in the flame retardant and melamine [3, 4].

S3. NMR analysis

Table S2. Sample composition used for NMR and DSC analysis. Sample composition was maintained same as used for composite preparation to simulation the actual condition.

Sample	Composition
DA	Pristine DA
Uncured_EPO	Pristine epoxy resin
Uncured_EPODA	Eopxy resin/DA = 2.6 (weight ratio), 5% DBU on the weight of DA
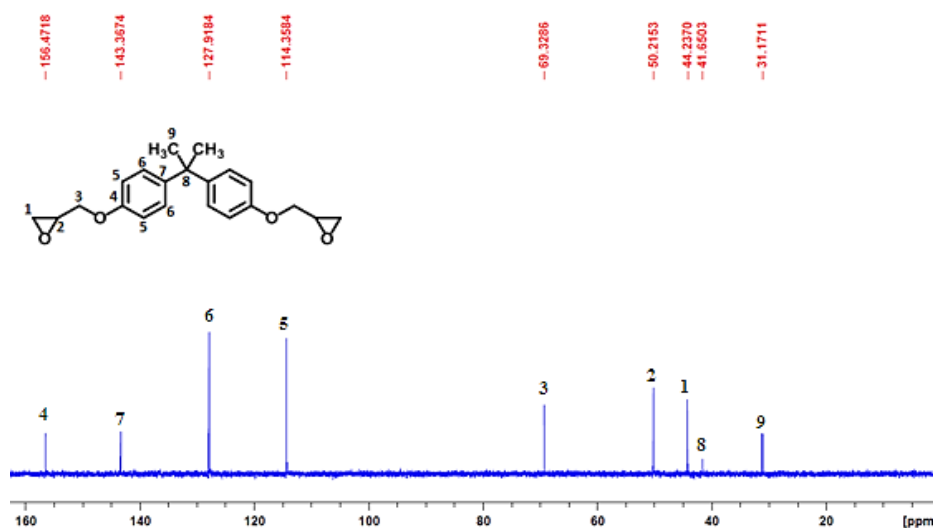
Fig. S2. ^{13}C-NMR spectrum of the sample composed of DBU, DA and pristine epoxy resin.
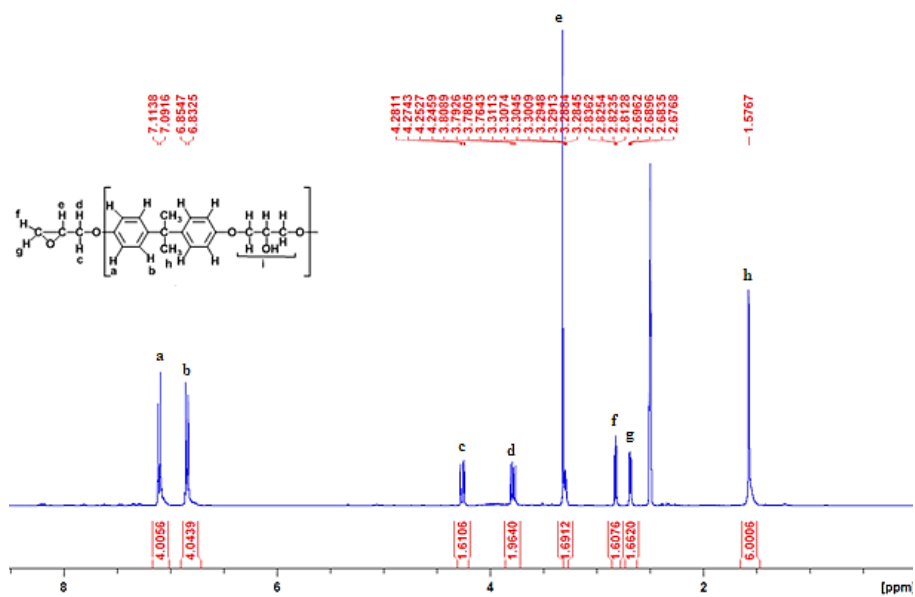
Fig. S3. ^{1}H-NMR spectrum of the sample with DBU, DA and epoxy resin. Peaks at 7.1 ppm and 6.8 ppm (aromatic protons) and 1.6 ppm (methylene protons) are characteristic of bisphenol A. The glycidyl terminal group is characterized by peaks in the range of 2.5–4.5 ppm (peaks c, d, e, f and g) [5].
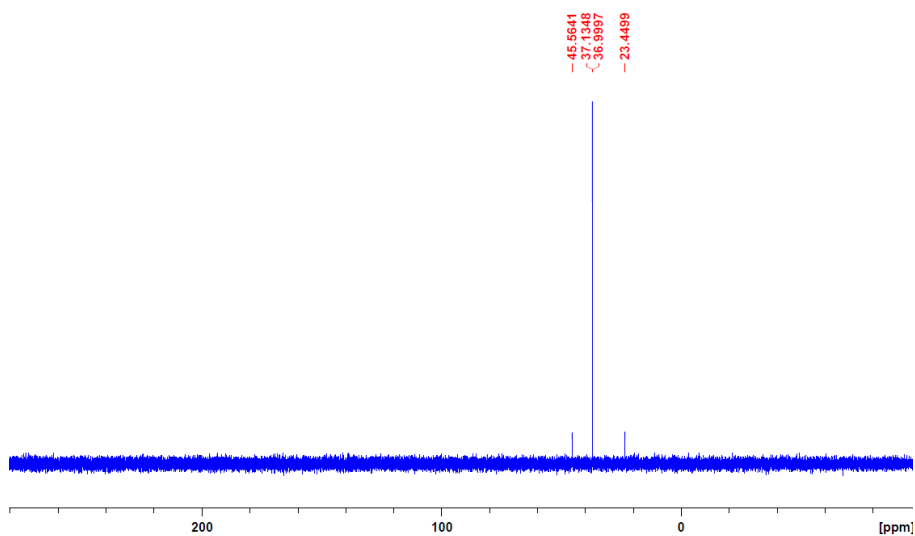
Fig. S4. ^{31}P-NMR spectrum of the sample composed by DBU, DA and pristine epoxy resin.

S4. Thermal analysis

Table S3. TGA analysis of all samples in air and N$_2$. T$_{5\%}$ is the temperatures at which 5 wt% loss was recorded. T$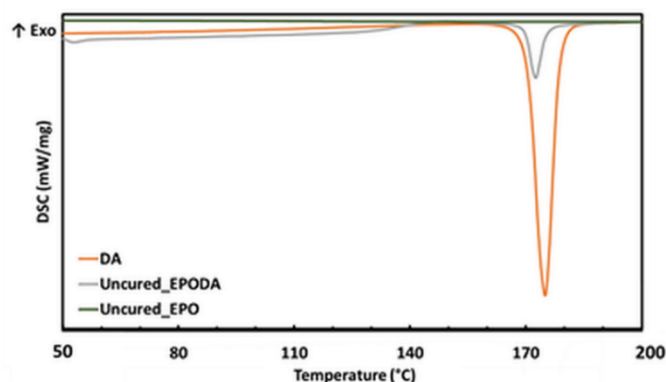_{max1}$, T$_{max2}$ and T$_{max3}$ are the temperatures at which the weight loss rate reached maximum; the residues at 800 °C is also reported.

Sample	T$_{5\%}$ (°C)	T$_{max1}$(°C)	T$_{max2}$ (°C)	T$_{max3}$ (°C)	Residue (wt%) at			
					T$_{max1}$	T$_{max2}$	T$_{max3}$	800 °C
Atmosphere: air								
EPO	336	351	519	-	75	18	-	0.7
DA2	275	351	526		64	33	-	3
Mel	250	279	351	509	83	58	24	2
DA2-Mel	237	277	364	534	82	57	20	3
Si2	293	367	553	-	61	11	-	1
Si-DA2	255	313	536	-	78	36	-	9
Si-Mel	241	274	354	531	83	61	21	2
Si-DA2-Mel	232	297	364	543	78	59	20	6
Si-DA-Mel	245	289	361	546	86	63	25	5
Atmosphere: N$_2$								
EPO	338	354	-	-	73	-	-	8
DA2	291	361	-	-	54	-	-	5
Mel	254	362	-	-	49	-	-	6
DA2-Mel	257	360	-	-	49	-	-	6
Si2	333	358	-	-	74	-	-	12
Si-DA2	283	362	-	-	57	-	-	9
Si-Mel	250	355	-	-	61	-	-	10
Si-DA2-Mel	239	363	-	-	52	-	-	9
Si-DA-Mel	242	326	-	-	66	-	-	12

Fig. S5. DSC curves (second heating cycles) of DA, **Uncured_EPODA (**mixture of pristine epoxy resin, DA and DBU) and **Uncured_EPO (**pristine epoxy resin). During DSC analysis samples were heated from 20 to 200 °C under N$_2$ (10 °C/min). The composition of measured samples is reported in Table S2.
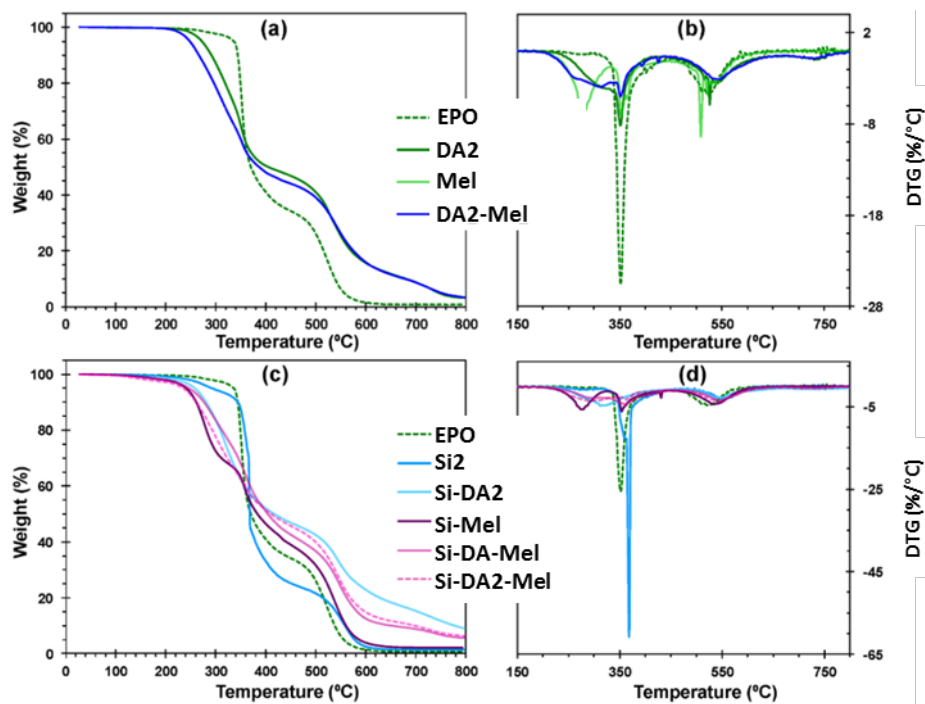
**Fig. S6.** TG (a-c) and DTG (b-d) curves of pristine epoxy (**EPO**) and epoxy composites recorded under air.

S5. Vertical flame spread tests

Table S4. Results of flame spread tests in vertical configuration.

Sample	UL 94 / Dripping	t_1 in Sec.					t_2 in Sec.				
EPO	Not classifiable (NC)/Yes				-						
DA1	NC/Yes				-						
DA2	V0/Yes	0	0	0	0	0	5	5	6	5	6
Mel	NC/Yes				-						
DA2-Mel	V0/Yes	0	0	0	0	0	4	3	2	3	2
Si2	NC/No				-						
Si-DA2	V0/No	5	6	4	5	4	4	4	6	5	6
Si-Mel	NC/No				-						
Si-DA2-Mel	V0/No	0	0	0	0	0	0	0	0	0	0
Si-DA-Mel	V1/No	4	3	3	4	3	11	12	11	13	12

t_1 and t_2 = Duration of flaming after 1st and 2nd flame application respectively.
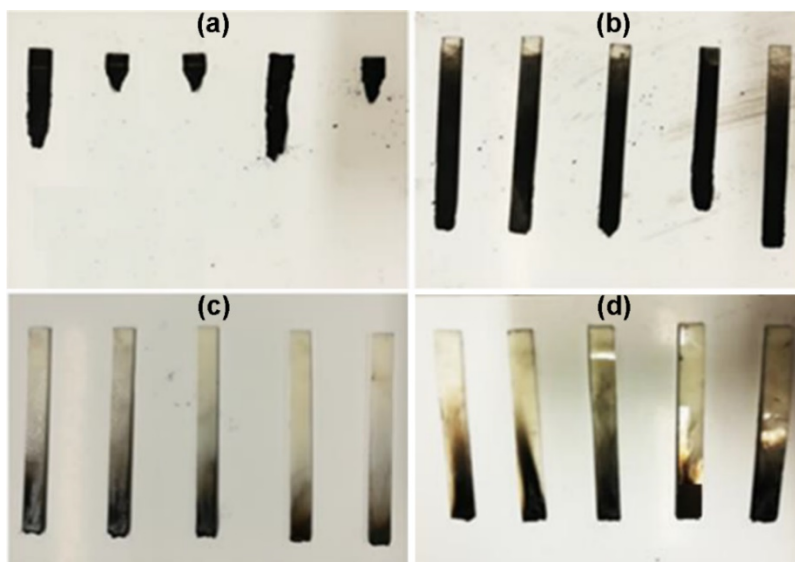
Fig. S7. Residues after UL-94 VB tests of (a) **EPO**, (b) **Si2**, (c) **DA2-Mel** and (d) **Si-DA2-Mel**.

S6. Pyrolysis combustion flow calorimetry results

Table S5. Pyrolysis Combustion Flow Calorimeter data for all the investigated samples.

Sample	THR (kJ/g)	HRC (J/g-K)	pHRR (W/g)	Residue (wt%)
EPO	30 ± 0.3	539 ± 44	545 ± 57	6 ± 0.2
DA2	29 ± 0.4	238 ± 11	238 ± 5	8 ± 0.4
Mel	29 ± 0.3	634 ± 102	496 ± 9	9 ± 0.8
DA2-Mel	30 ± 0.5	271 ± 15	271 ± 11	8 ± 0.7
Si2	28 ± 0.1	450 ± 23	448 ± 22	11 ± 0.9
Si-DA2	28 ± 0.1	259 ± 11	259 ± 12	10 ± 0.5
Si-Mel	26 ± 0.7	393 ± 14	393 ± 7	9 ± 0.6
Si-DA-Mel	28 ± 0.4	345 ± 32	302 ± 16	10 ± 0.9
Si-DA2-Mel	27 ± 0.1	306 ± 5	245 ± 2	9 ± 0.7

THR = Total Heat Release, **HRC** = Heat Release Capacity, **pHRR** = peak of Heat Release Rate.

S7. Cone calorimetry tests and calculation of Flame Retardancy Index, Flame Propagation Index and Time To Flashover.
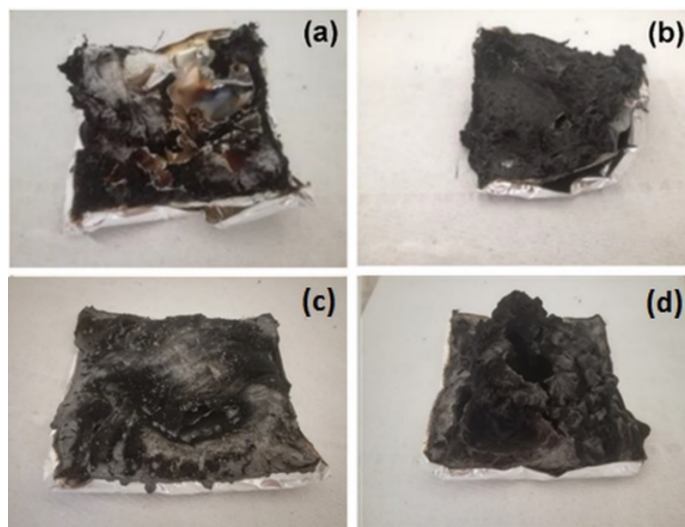
Fig. S8. Photograph of the char residues obtained after cone calorimetry tests for (a) **EPO**, (b) **Si2,** (c) **DA2** and (d) **Si-DA2-Mel.** DA and silica nanoparticles act in the condensed phase through the formation of a coherent char (b-c), while the presence of melamine guarantees an evident intumescence (d).

Fig. S9. Capture frame from the video recording the formation of a swollen multicellular carbonaceous layer in the cone calorimetry test for **Si-DA2-Mel**.

Table S6. Results from cone calorimetry tests for the investigated samples.

Sample	TTI (s)	TTFO (s)	THR (MJ/m^2)	MLR (g/s·m^2)	HRR (kW/m^2)	pHRR (kW/m^2)	Residue (wt%)	FPI	TTF (min)	FRI
EPO	38±3	117± 3	96±3	77±3	532±23	2550±384	1±0.7	67	-	-
DA2	34±1	200±0.5	43±3	30±2	160±20	647±81	3±0.6	19	3	7.9
DA2-Mel	50±6	206±5	61±6	31±5	238±18	806±124	3±0.5	16	4	6.6
Si2	40±4	130±5	79±10	42±4	412±11	1964±73	4±0.5	49	-	1.7
Si-DA2	26±5	158±5	63±7	32±5	276±10	773±108	5±0.7	30	1	3.4
Si-DA2-Mel	56±4	189±3	59±7	35±3	249±13	823±102	4±0.6	14	4	7.5

TTI = Time To Ignition, **TTFO** = Time To Flame Out, **THR** = Total Heat Release, **MLR** = Mass Loss Rate, **HRR** = Heat Release Rate, **pHRR** = peak of Heat Release Rate, **FPI =** Flame Propagation Index, **TTF** = Time To Flashover, **FRI**= Flame Retradancy Index. FRI is not reported for **EPO**, because this sample represents the neat polymer.

Flame retardant index was calculated using eq. 1 reported by Movahedifar et al. [6, 7]. This index is calculated using the cone calorimeter data of pristine epoxy resin (EPO) and flame retardant composites developed in this work (Table S6).

$$\text{Flame Retardancy Index } = \frac{\left[\text{THR} \cdot \left(\frac{\text{pHHR}}{\text{TTI}}\right)\right]_{\text{Neat Polymer}}}{\left[\text{THR} \cdot \left(\frac{\text{pHHR}}{\text{TTI}}\right)\right]_{\text{Composite}}} \tag{1}$$

On the other side, TTF was calculated according using eq to the formulas reported by Lyon et al. [8] as follow:

$$\text{Flame Propagation Index (FPI)} = \frac{\text{pHRR}}{\text{TTI}} \tag{2}$$

$$\text{Time To Flashover (TTF)} = 991 - 629 \cdot \log_{10} \text{FPI} \tag{3}$$

Flashover is a very important phenomenon which occurs in the case of compartment fires where incomplete combustion products accumulate at the ceiling and ignite causing total involvement of the compartment materials and signaling the end to human survivability. Therefore, TTT represents the time available for escape and this is the single most important factor in determining the fire hazard. The equation (3) used to calculate the TTF presupposes the knowledge of the FPI [8]. Equation (3) provided the best fit (r^2= 0.94) to all of the EURIFIC full-scale fire test data [9] for 13 different lining materials obtained according to ISO9705 corner wall/room fire test using the 100/300 ignition option (100 kW fire for 10 minutes +300 kW fire for additional 10 minutes) in the corner of a 3.6-m-long x 2.4-m-wide by 2.4-m-high room [8, 9].
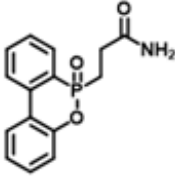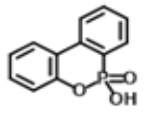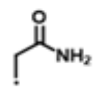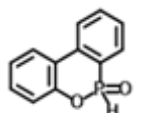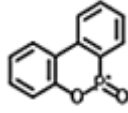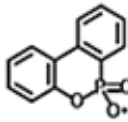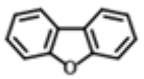
Table S7. Smoke parameters from cone calorimetry tests for the investigated samples.

Sample	TSR (m²/m²)	SEA (m²/kg)	CO yield (kg/kg)	CO₂ yield (kg/kg)	CO/CO₂
EPO	1841± 206	131± 35	0.03± 0.003	0.4± 0.06	0.08
DA2	4237± 216	524± 30	0.06± 0.0003	0.4± 0.05	0.15
DA2-Mel	4254± 225	526± 22	0.07± 0.003	0.5± 0.04	0.14
Si2	1981± 290	241± 38	0.03± 0.004	0.7± 0.02	0.04
Si-DA2	4626± 304	576± 75	0.08± 0.007	0.5± 0.2	0.16
Si-DA2-Mel	4108± 275	508± 3	0.08± 0.003	0.5± 0.02	0.16

TSR = Total Smoke Release, SEA = Smoke Extension Area.

S8. Pyrolysis–Gas Chromatography–Mass and Direct Insertion Probe–Mass Spectrometry

Table S8. Major decomposition products of DA [2].

Compound	m/z	Symbol	Compound	m/z	Symbol
	287	F		232	N
	72	G		216	L
	215	M		48	Q
	231	O		168	P
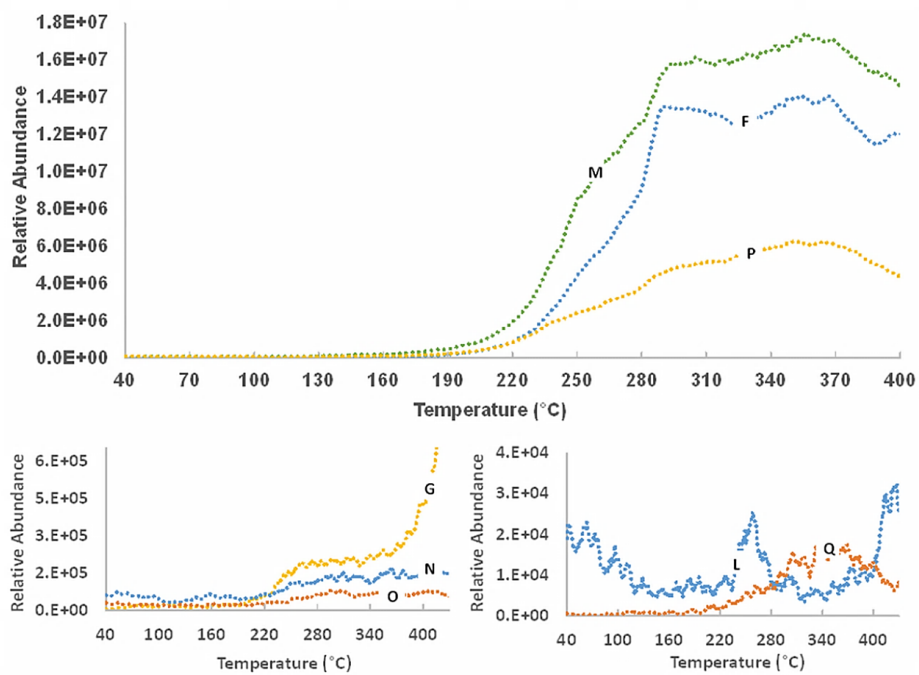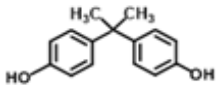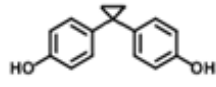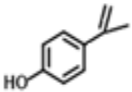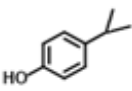
Fig. S10. DIP-MS analysis of **Si-DA2-Mel**, thermograms of its major decomposition species listed in Table S8.
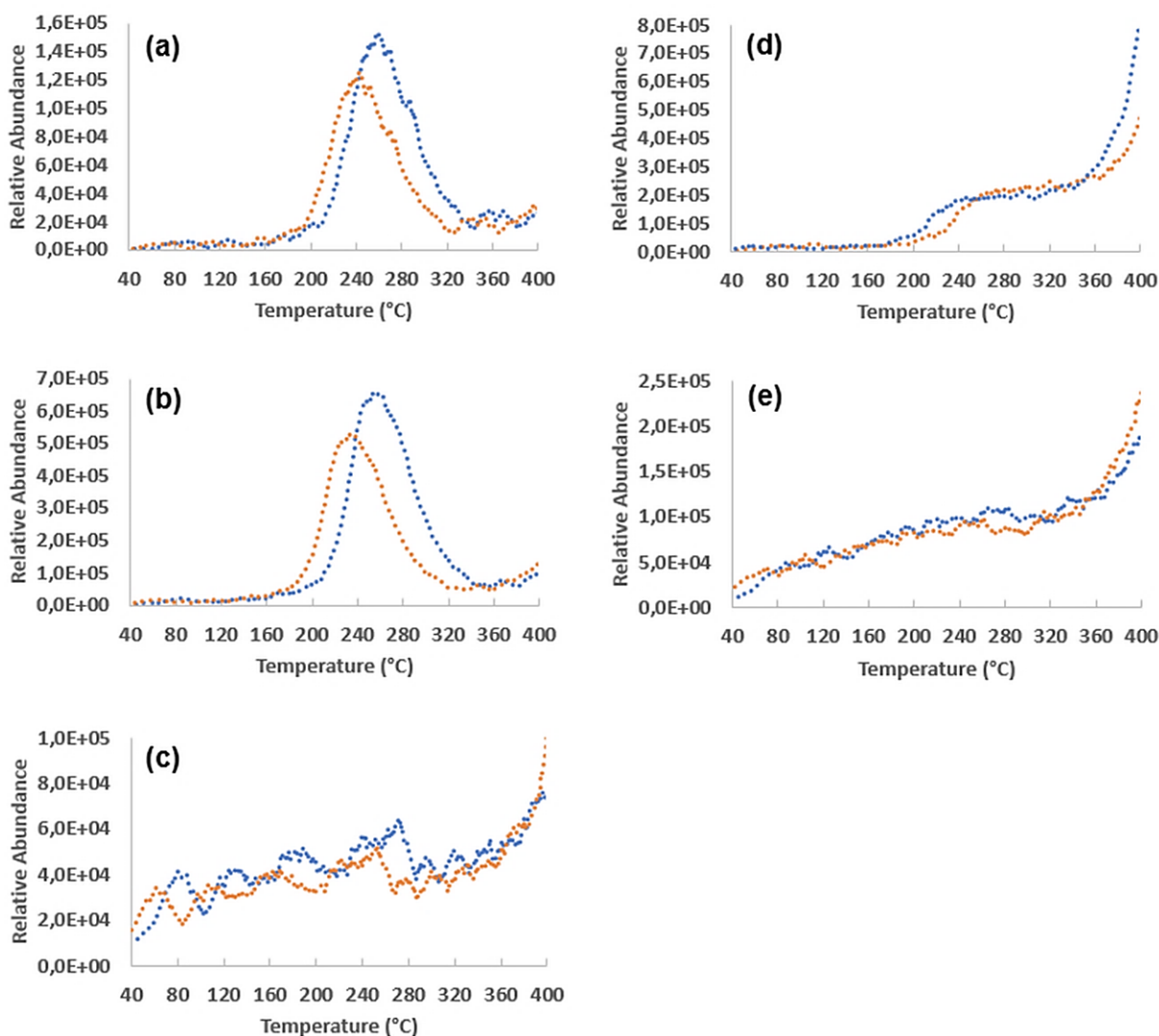
Fig. S11. DIP-MS analysis of **EPO (blue)** and **Si-DA2-Mel (orange)**, thermograms of their major decomposition species listed in Table S9: bisphenol A (a), 4,4'-(cyclopropane-1,1-diyl)di-phenol (b), phenol (c), 4-isopropenylphenol (d), 4-isopropylphenol (e).

Table S9. Major decomposition products of pristine epoxy with cycloaliphatic hardener under N_2 atmosphere [10-18].

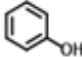| Compound	m/z	Name	Symbol
	228	bisphenol A	A
	226	4,4'-(cyclopropane-1,1-diyl)diphenol	B
	94	phenol	C
	134	4-isopropenylphenol	D
	136	4-isopropylphenol	E

Scheme S1. The proposed mechanism of **EPO**/DA reactions in oxygen (O_2) atmosphere.
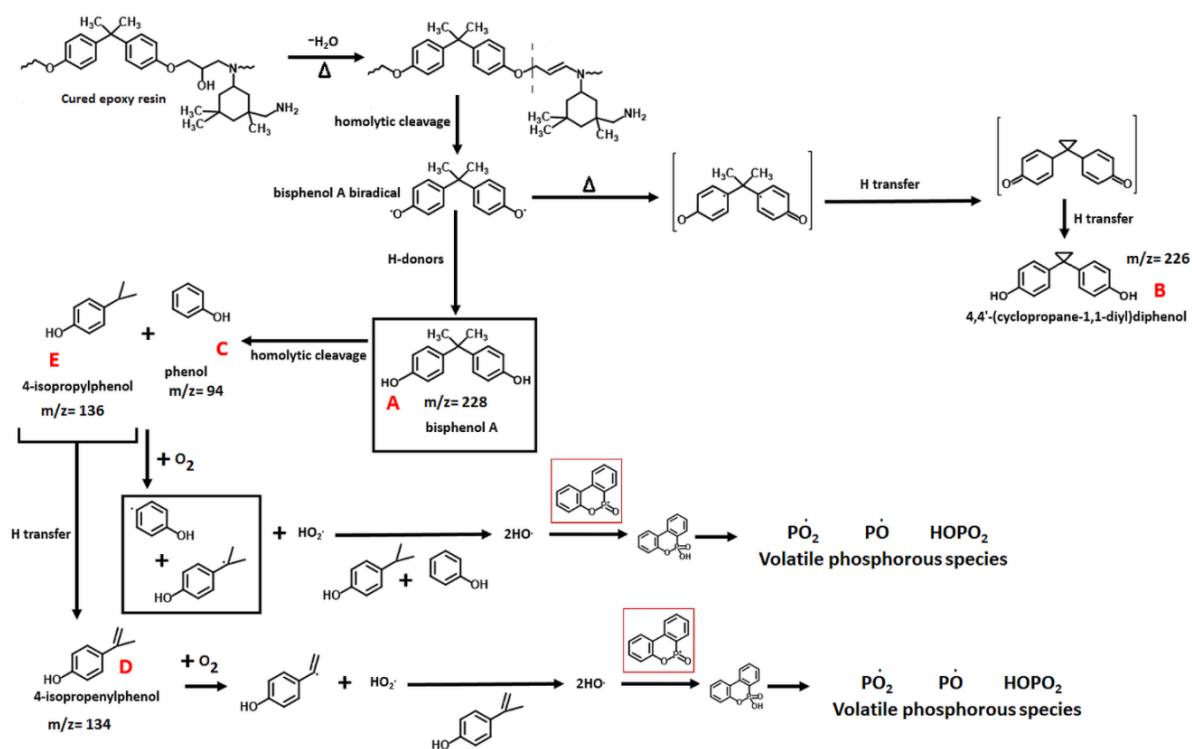
S9. FTIR and EDX analysis of char
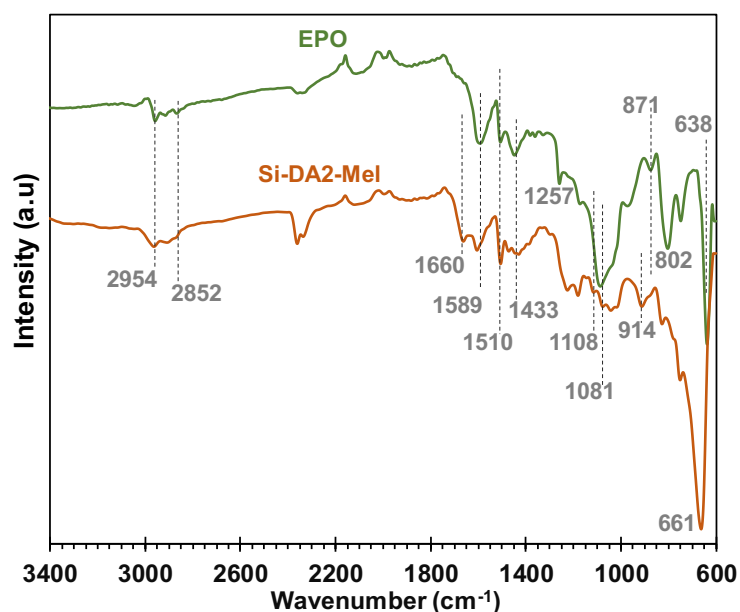
Fig. S12. Full scale FTIR spectra of char obtained after vertical burning test of **EPO** and **SI-DA2-Mel.**

Fig. S12 show that in case of char formed from neat epoxy (**EPO**), peaks at 638 cm^{-1}, 802 cm^{-1} and 871 cm^{-1} are due to aromatic C–H stretching in meta, para and ortho, respectively [3, 19]. The combustion of diglycidyl ether of bisphenol A (DGEBA) epoxy resin produces molecules containing alkoxy C–O and phenol C–O groups with stretching bands at 1081 cm^{-1} and 1257 cm^{-1} respectively [3, 20]. The band around 1433 cm^{-1} may be due to the presence of P–N stretching vibrations in the char [3]. The band at 1510 cm^{-1} may be attributed to the stretching vibrations of aromatic carbons [3, 4]. The bands at 2852 cm^{-1} and 2954 cm^{-1} correspond to the stretching vibration of the C–H.

S10. Mechanical behavior

Table S10. Tensile tests result of pure epoxy resin (**EPO**) and epoxy nanocomposites for comparison. The tensile modulus was calculated from the slope strain range below 0.2% and all the curves are linear until the fracture breaking point, without plastic deformation.

Sample	E_t (MPa)	$\sigma_{u,t}$ (MPa)	$\varepsilon_{f,t}$ (%)	U_T (J/m^3)
EPO	2629 ± 42	112 ± 35	4.2 ± 1.2	2162
Si2	2896 ± 24	89 ± 27	3.1 ± 0.9	1121
Si-DA2-Mel	3426 ± 15	77 ± 22	2.4 ± 0.7	461

Table S11. Results from three-point bending flexural tests for pure epoxy resin, in-situ silica-epoxy system and the in-situ silica-resin added of melamine and DA (2 wt% of P).

Sample	E_B (MPa)	$\sigma_{u,B}$ (MPa)	$\varepsilon_{f,B}$ (%)
EPO	2642 ± 468	106 ± 12	6.2 ± 0.6
Si2	2920 ± 14	92 ± 15	3.4 ± 0.8
Si-DA2-Mel	3545 ± 276	76 ± 4	2.6 ± 0.1

References

1. X. Liu, K.A. Salmeia, D. Rentsch, J. Hao, S. Gaan, Thermal decomposition and flammability of rigid PU foams containing some DOPO derivatives and other phosphorus compounds, J. Anal. Appl. Pyrolysis. 124 (2017) 219–229.

2. K.A. Salmeia, A. Gooneie, P. Simonetti, R. Nazir, J.-P. Kaiser, A. Rippl, C. Hirsch, S. Lehner, P. Rupper, R. Hufenus, Comprehensive study on flame retardant polyesters from phosphorus additives, Polym. Degrad. Stab. 155 (2018) 22–34.

3. K.A. Salmeia, A. Neels, D. Parida, S. Lehner, D. Rentsch, S. Gaan, Insight into the Synthesis and Characterization of Organophosphorus-Based Bridged Triazine Compounds, Molecules. 24 (2019) 2672.

4. R.R. Randle, D.H. Whiffen, The infra-red intensities of a band near 1020 cm^{-1} in mono- and para-substituted benzene derivatives, Trans. Faraday Soc. 52 (1956) 9–13.

5. F.G. Garcia, B.G. Soares, Determination of the epoxide equivalent weight of epoxy resins based on diglycidyl ether of bisphenol A (DGEBA) by proton nuclear magnetic resonance, Polym. Test. 22 (2003) 51–56.

6. H. Vahabi, B.K. Kandola, M.R. Saeb, Flame retardancy index for thermoplastic composites, Polymers 11 (2019) 407.

7. E. Movahedifar, H. Vahabi, M.R. Saeb, S. Thomas, Flame retardant epoxy composites on the road of innovation: an analysis with flame retardancy index for future development, Molecules 24 (2019) 3964.

8. R.E. Lyon, U. Sorathia, P.N. Balaguru, A. Foden, J. Davidovits, M. Davidovits, in: The First International Conference on Composites in Infrastructure (ICCI' 96), Fire response of geopolymer structural composites, U.S. Department of Transportation, Tuscon, 1996, pp. 972-981.

9. B. Karlsson, S.E. Magnusson, in: Fire Safety Science - Proceedings of the Third International Symposium, Combustible wall lining materials: Numerical simulation of room fire growth and the outline of a reliability based classification procedure, Department of Fire Safety Engineering – Lund University, Sweden, 1991, pp. 667-678.

10. D. Braun, W. Von Gentzkow, A.P. Rudolf, Hydrogenolytic degradation of thermosets, Polym. Degrad. Stab. 74 (2001) 25–32.

11. H. Yan, C. Lu, D. Jing, X. Hou, Chemical degradation of TGDDM/DDS epoxy resin in supercritical 1-propanol: Promotion effect of hydrogenation on thermolysis, Polym. Degrad. Stab. 98 (2013) 2571–2582.

12. K. Shirokane, T. Wada, M. Yoritate, R. Minamikawa, N. Takayama, T. Sato, N. Chid, Total Synthesis of (±)-Gephyrotoxin by Amide-Selective Reductive Nucleophilic Addition, Angew. Chemie Int. Ed. 53 (2014) 512–516.

13. H. Yan, C. Lu, D. Jing, X. Hou, Chemical degradation of amine-cured DGEBA epoxy resin in supercritical 1-propanol for recycling carbon fiber from composites, Chinese J. Polym. Sci. 32 (2014) 1550–1563.

14. S. V Levchik, G. Camino, M.P. Luda, L. Costa, G. Muller, B. Costes, Epoxy resins cured with aminophenylmethylphosphine oxide—II. Mechanism of thermal decomposition, Polym. Degrad. Stab. 60 (1998) 169–183.

15. W. Chin, M. Shau, W. Tsai, Synthesis, structure, and thermal properties of epoxy-imide resin cured by phosphorylated diamine, J. Polym. Sci. Part A Polym. Chem. 33 (1995) 373–379.

16. M. Shau, T. Wang, Syntheses, structure, reactivity, and thermal properties of new cyclic phosphine oxide epoxy resins cured by diamines, J. Polym. Sci. Part A Polym. Chem. 34 (1996) 387–396.

17. W. Zhang, A. Fina, G. Ferraro, R. Yang, FTIR and GCMS analysis of epoxy resin decomposition products feeding the flame during UL 94 standard flammability test. Application to the understanding of the blowing-out effect in epoxy/polyhedral silsesquioxane formulations, J. Anal. Appl. Pyrolysis 135 (2018) 271-280.

18. B. Schartel, Phosphorus-based flame retardancy mechanisms—old hat or a starting point for future development?, Materials (Basel). 3 (2010) 4710–4745.

19. R. Jian, P. Wang, W. Duan, J. Wang, X. Zheng, J. Weng, Synthesis of a novel P/N/S-containing flame retardant and its application in epoxy resin: thermal property, flame retardance, and pyrolysis behavior, Ind. Eng. Chem. Res. 55 (2016) 11520–11527.

20. P. Musto, Two-Dimensional FTIR spectroscopy studies on the thermal-oxidative degradation of epoxy and epoxy− bis (maleimide) networks, Macromolecules. 36 (2003) 3210–3221.